Improved Sensing Characteristics of a Novel Pt/$HfTiO_2$/SiC Schottky-Diode Hydrogen Sensor

W. M. Tang, C. H. Leung, and P. T. Lai, *Senior Member, IEEE*

***Abstract*—A novel metal–insulator–silicon carbide Schottky-diode hydrogen sensor with $HfTiO_2$ gate insulator annealed in three different gases (N_2, O_2, or NO) is fabricated. Measurements are carried out at various hydrogen concentrations at high temperature using a computer-controlled measurement system. The hydrogen-sensing characteristics of the devices are studied with the help of ellipsometry, transmission electron microscopy, scanning electron microscope, energy-dispersive spectroscopy, and atomic force microscopy. Experimental results show that these sensors have high sensor output and can give significant response even at low hydrogen concentration. This work also finds that the NO-annealed sensor has the highest sensor output. When 800-ppm H_2 in N_2 gas is introduced, the NO-annealed sensor exhibits a high sensor output of 782% at 450 °C, which is about three and six times higher than those of the O_2- and N_2-annealed sensors, respectively. As compared to another sensor with HfO_2 gate insulator annealed in NO, the proposed NO-annealed sensor shows higher sensor output, which should be mainly attributed to the larger barrier height at the metal–insulator interface. The excellent hydrogen-sensing characteristics of this novel sensor make it very suitable for detecting hydrogen leakage, particularly in high-temperature environments.**

***Index Terms*—Annealing, $HfTiO_2$, Schottky diode, SiC-based hydrogen sensor.**

I. Introduction

HYDROGEN is widely used in our daily life. It is a colorless and odorless gas and is less dense than air. It was first identified and characterized by an English chemist Henry Cavendish in 1766 [1]. It can be produced by a variety of methods, including acid and iron methods, steam-reforming production method, coal and electrolysis methods, biological processes, and chemical decomposition of hydrogen-containing compounds. However, it is a very dangerous gas because it can cause a serious explosion if a spark is present. It can also make various metals such as high-strength steels, nickel and titanium alloys become brittle and crack. In order to avoid the leakage of hydrogen that can cause serious accidents, sensors that can detect hydrogen quickly and accurately are very important and essential in practical applications. Apart from leak detection, monitoring of the hydrogen or hydrocarbon concentration in fuel cells, hydrogen-driven vehicles, car exhaust, flues, and biomedical and chemical industries is also an important application of hydrogen sensors.

There are various types of hydrogen sensors which use different sensing mechanisms to detect hydrogen. Many of them use catalytic metals such as palladium (Pd) or platinum (Pt) as a hydrogen trap because these metals have high hydrogen solubility and can selectively absorb hydrogen gas. There are many types of hydrogen sensors such as pyroelectric sensors, piezoelectric sensors, fiber-optic sensors, electrochemical sensors, and semiconductor sensors. Among the various types of sensors, semiconductor sensors are preferably selected as gas sensors due to their much simpler electronic circuitry required for operation. The detection of hydrogen gas with semiconductor sensors is primarily done with semiconductor metal oxides. The initial work on this type of sensor can be traced back to the work of Brattain and Bardeen [2] in 1953. The sensing properties of this sensor are based on reactions between semiconductor oxides and gases in the atmosphere. There is another category of semiconductor hydrogen sensor in which the species of interest are absorbed at semiconductor interfaces and induce interfacial polarization. The first hydrogen sensor under this category was developed by Lundstrom *et al.* in 1975 [3] and was a metal–oxide–semiconductor (MOS) structure using silicon as substrate, silicon dioxide as gate insulator, and palladium as gate electrode. Since then, a lot of research on such hydrogen sensors has been done. Different materials and fabrication methods have been used to make the hydrogen sensors [4]. Silicon carbide (SiC), a wide-bandgap material, is commonly used to make the hydrogen sensor because it can operate potentially up to 1000 °C. The recent focus of SiC-based gas sensors has been on metal–insulator–SiC (MISiC) gas sensors because these sensors can have better sensitivity, stability, and selectivity [5]. Silicon oxynitride (SiON) has been used as gate insulator for fabricating MISiC Schottky-diode hydrogen sensors [6], [7]. It can suppress leakage current and reduce interface states and oxide charges and hence improve the sensor performance. Apart from oxynitrides, high-k metal oxides can also be used as the gate insulator for reduced leakage. Many high-k metal oxides such as Al_2O_3 [8], Y_2O_3 [9], La_2O_3 [10], ZrO_2 [11], TiO_2 [12], Ta_2O_3 [13], and HfO_2 [14] have been investigated during the last decade for potential replacement of SiO_2 as gate dielectrics in complementary MOS (CMOS)-based VLSI circuits. There are several methods to produce the high-k film such as atomic layer deposition, electron-beam evaporation,

Manuscript received March 5, 2012; revised July 11, 2012; accepted July 13, 2012. Date of publication August 24, 2012; date of current version September 18, 2012. This work was supported in part by the RGC of Hong Kong under Project HKU 713310E and in part by the University Development Fund (Nanotechnology Research Institute) of The University of Hong Kong under Grant 00600009. The review of this paper was arranged by Editor J. D. Cressler.

W. M. Tang was with the Department of Electrical and Electronic Engineering, The University of Hong Kong, Pokfulam, Hong Kong. She is now with Stanford University, Stanford, CA 94305 USA (e-mail: wmtang@eee.hku.hk).

C. H. Leung and P. T. Lai are with the Department of Electrical and Electronic Engineering, The University of Hong Kong, Pokfulam, Hong Kong (e-mail: chleung@eee.hku.hk; laip@eee.hku.hk).

Color versions of one or more of the figures in this paper are available online at http://ieeexplore.ieee.org.

Digital Object Identifier 10.1109/TED.2012.2209430

sol–gel deposition, dc or RF sputtering, and molecular beam epitaxy. Of these deposition methods, dc and RF sputterings are generally preferred because they allow low-temperature processing and can easily make films with different compositions and microstructures.

In this work, a novel MISiC Schottky-diode hydrogen sensor with $HfTiO_2$ as gate insulator is fabricated for investigation. $HfTiO_2$ is a promising gate dielectric for future CMOS technology because incorporating Ti into hafnium oxide can increase the dielectric constant of Hf-based oxide [15]–[17]. The hydrogen-sensing properties of the device are studied and compared with those of its counterpart based on HfO_2 by taking measurements at various hydrogen concentrations at high temperature using a computer-controlled measurement system. The qualities, structures, and compositions of the devices are studied by ellipsometry, transmission electron microscopy (TEM), scanning electron microscope (SEM), energy-dispersive spectroscopy (EDX), and atomic force microscopy (AFM).

II. Experiments

An n-type (0001) Si-face 4H–SiC wafer, manufactured by CREE research, was used in this study. The SiC wafer had a 5-μm epitaxial layer grown on a heavily doped substrate. The doping level of the epitaxial layer was $5-6 \times 10^{15}$ cm^{-3}. The wafer was cleaned using the conventional RCA method, followed by a 60-s dip in 5% hydrofluoric acid to remove the native oxide. The wafer was then loaded into a Denton Vacuum LLC Discovery 635 sputterer, which was then pumped down to 2×10^{-6} torr. $HfTiO_2$ was then deposited at room temperature by cosputtering of hafnium metal (99.99% purity) with an RF power of 25 W and titanium metal (99.995% purity) with a dc current of 0.1 A in a mixed Ar/O_2 ambient (Ar-to-O_2 ratio $=$ 8 : 1) for 12.3 min. An electrode consisting of 100-nm Pt with a diameter of 0.5 mm was then deposited on the wafer by dc magnetron sputtering through a stainless steel shadow mask. The sample then underwent an annealing in a furnace at 650 °C in N_2 (1000 mL/min) for 10 min (denoted as N2 sample). In order to investigate the effects of annealing gas on the sensor performance, two more hydrogen sensors annealed under the same annealing temperature and duration but in different annealing gases were fabricated. The samples annealed in O_2 and NO were denoted as O2 and NO, respectively. The samples were pasted on headers using silver epoxy. The headers were then put into an oven at 200 °C for half an hour to harden the silver epoxy. Finally, a gold wire was connected between the front electrode and one of the pins of the header using a hybrid wedge bonder. The hydrogen sensor fabricated in this study is shown in Fig. 1. The processing conditions and insulator thickness of each sample are summarized in Table I. After the fabrication of the sensors, their hydrogen-sensing properties were investigated and compared with those of the sensor based on HfO_2. The details of the fabrication process of the HfO_2-based sensor were discussed elsewhere [18]. Measurements were carried out using a computer-controlled measurement system as shown in Fig. 2. Three devices were measured simultaneously for each type of hydrogen sensors. The humidity of the laboratory was maintained at 50% during measurements.

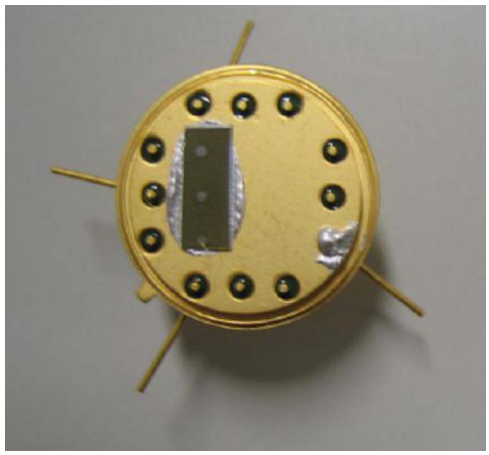

Fig. 1. Sensor chip bonded to an IC header.

TABLE I
PROCESSING CONDITIONS AND INSULATOR THICKNESS OF EACH SAMPLE

Device	N2	O2	NO
Insulator	$HfTiO_2$	$HfTiO_2$	$HfTiO_2$
Annealing gas	N_2	O_2	NO
Annealing temperature (°C)	650	650	650
Annealing time (min)	10	10	10
Insulator thickness (nm)	4.10	4.06	4.30

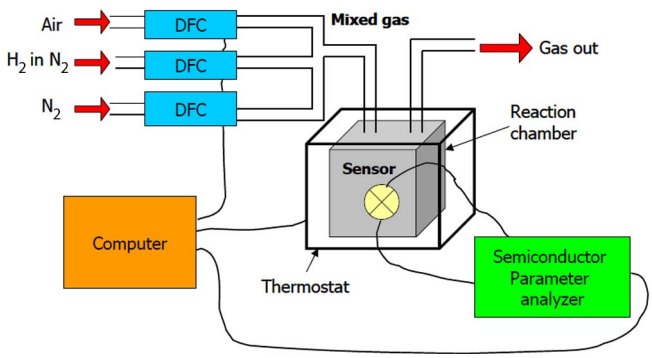

Fig. 2. Computer-controlled measurement system.

III. Results and Discussion

Fig. 3 shows the TEM images of the (a) N2 and (b) NO samples. The graph clearly shows the crystal structure of the SiC substrate and a very thin insulator layer in the cross section of the device. Epoxy is shown in the TEM image as it is used during the TEM sample preparation to attach the front sides of the two samples together. Since the Pt layer is deposited onto the insulator layer only in the form of dots with a diameter of 0.5 mm, the Pt layer cannot be seen in the cross section of the sample shown in Fig. 3(b). Fig. 4 shows the SEM picture of the N2 sample. As the catalytic metal electrode is the most important part of the Schottky-diode hydrogen sensors where dissociative reactions of hydrogen take place, the composition

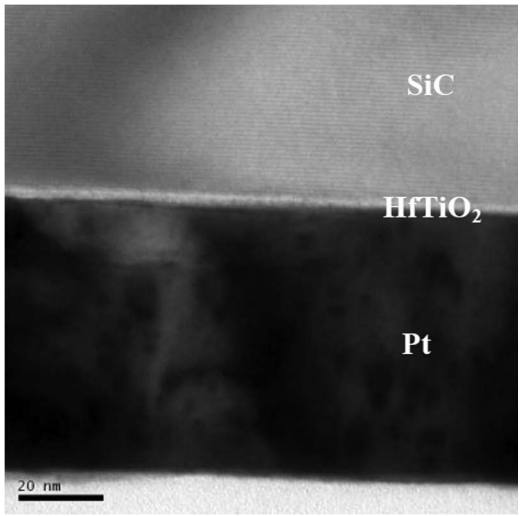

(a)

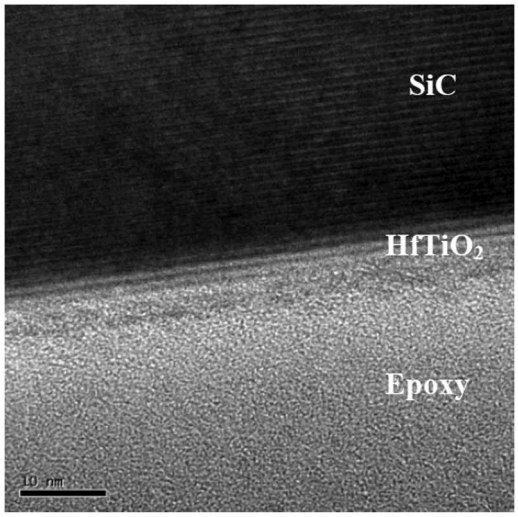

(b)

Fig. 3. TEM images of the (a) N2 sample and (b) NO sample.

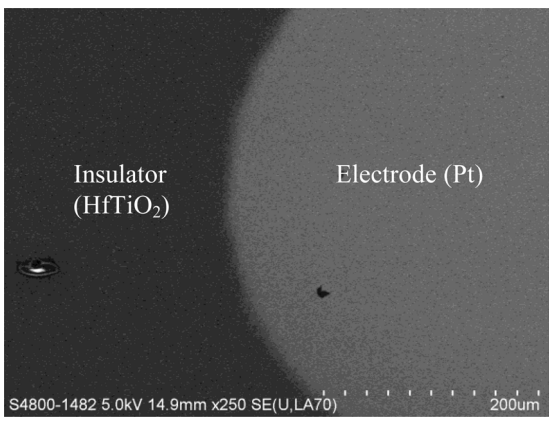

Fig. 4. SEM image of the N2 sample.

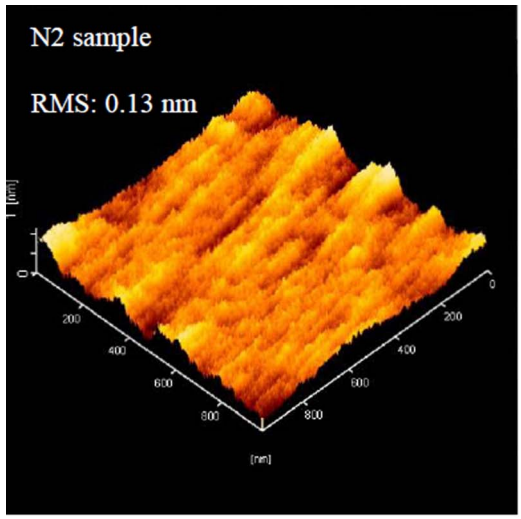

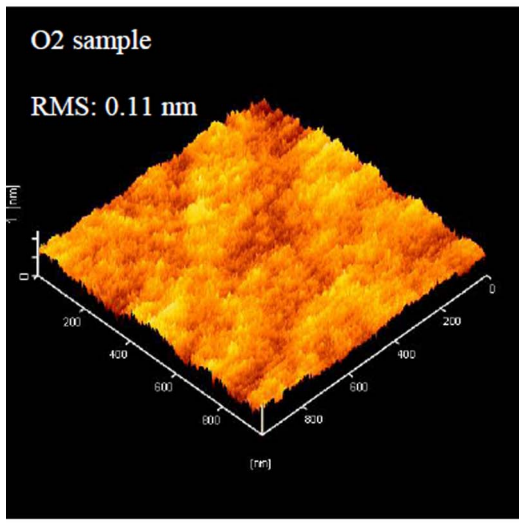

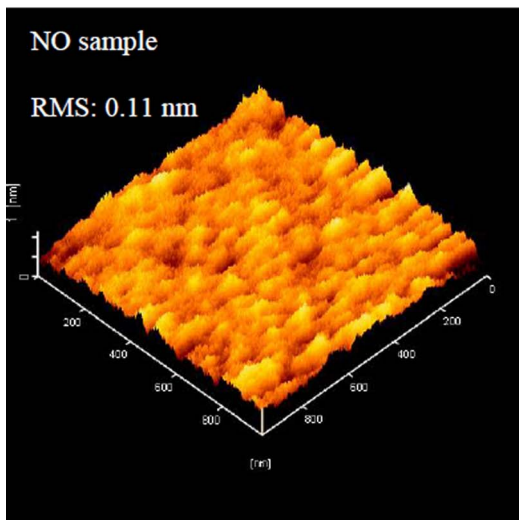

Fig. 5. AFM images of the samples.

of the electrode is then examined by EDX coupled with the SEM measurement tool. The results confirm that the electrode consists of platinum.

Surface roughness and surface morphology of a film are important physical properties which may affect the electrical properties of electron devices and their sensing capability [19]–[22]. The morphologies of the $HfTiO_2$ films annealed in N_2, O_2, and NO shown in Fig. 5 are characterized by an AFM machine (SII Nanopics 2100). The AFM images show that all the films have a densely packed amorphous structure, and AFM measurements reveal the rms roughness of the films shown in the figures. It is found that all the films have a smooth surface with an rms

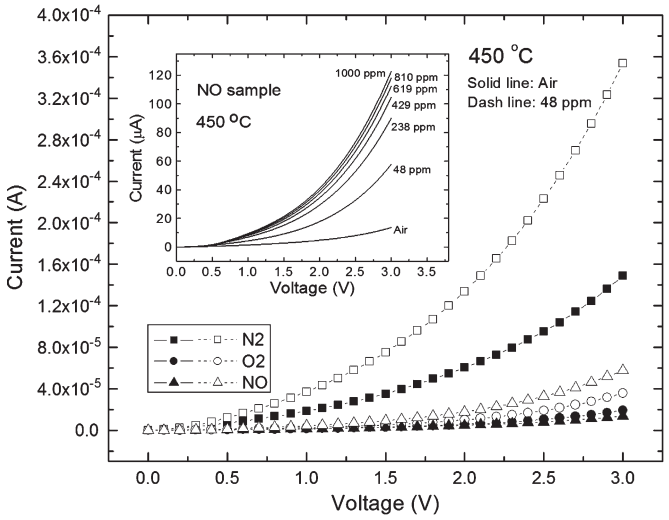

Fig. 6. I–V curves of the samples in air and in 48-ppm H_2 in N_2 at 450 °C. The inset shows the I–V curves of the NO sample at different H_2 concentrations.

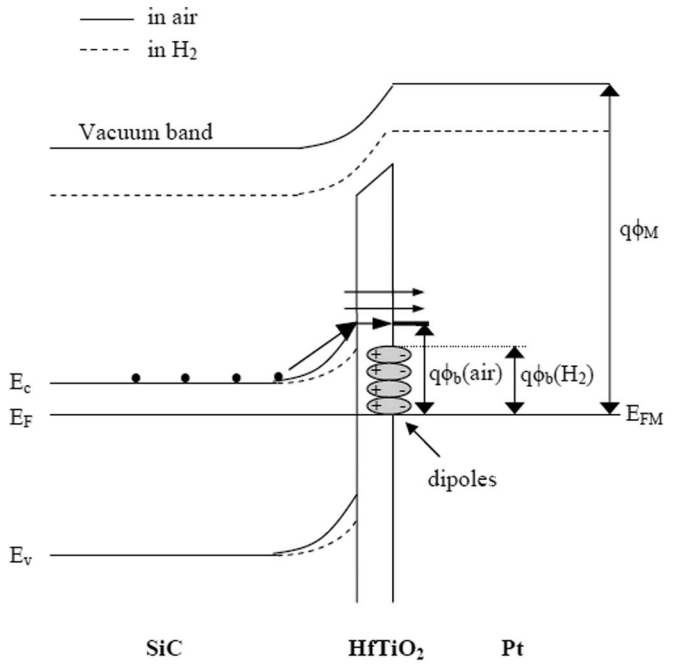

Fig. 7. Schematic energy-band diagram for a MISiC Schottky-diode hydrogen sensor.

roughness within 0.11–0.13 nm. As all the studied $HfTiO_2$ films exhibit similar physical characteristics in terms of morphology and roughness, the differences in the sensing performance of the studied devices (as shown in the following) are thus mostly attributed to the difference in the interfacial and dielectric properties of the devices rather than the surface properties of the dielectric films.

The I–V characteristics of the fabricated sensors in air and in hydrogen environment have been studied and are shown in Fig. 6. The I–V curves shift to the left upon exposure to 48-ppm H_2 in N_2. The inset of Fig. 6 shows the I–V curves of the NO sample measured in air and in different H_2 concentrations (48, 238, 429, 619, 810, and 1000 ppm). The I–V curve shifts to the left as the hydrogen concentration increases. When hydrogen molecules come to the catalytic gate metal, they dissociate at the surface of the metal and form hydrogen atoms. These hydrogen atoms then diffuse through the metal on the order of nano- to microseconds to the insulator surface and become polarized due to the displacement of their negatively charged electron cloud relative to their positively charged nucleus induced by an external applied field. This dipole layer causes a shift of the electrical (I–V) characteristics of the devices. The amount of voltage shift at a fixed current is assumed to be proportional to the atomic hydrogen concentration at the interface or the hydrogen coverage θ_i. The maximum voltage change $\Delta V_{\max}$ occurs when each hydrogen absorption site at the interface is occupied by one hydrogen atom, i.e., the hydrogen coverage is one. Fig. 7 shows the schematic energy-band diagram of a MISiC Schottky-diode hydrogen sensor. Electrons in the conduction band of the substrate (SiC) have to overcome an energy barrier ϕ_b to reach the gate (Pt). The polarized hydrogen layer can increase the electron concentration of the metal and, hence, its Fermi level near the insulator layer. As a result, the reduced energy barrier at the metal–insulator interface increases the forward current of the device.

Based on the thermionic-emission conduction mechanism of a Schottky diode, for forward bias $V > 3kT/q$, its I–V characteristics are given by [23]

$$I = I_o \exp\left(\frac{qV}{nkT}\right) \tag{1}$$

where k is the Boltzmann constant, T is the temperature in Kelvin, and n is the ideality factor. I_o is the saturation current defined as

$$I_o = AA^{**}T^2 \exp\left(-\frac{\phi_b}{\phi_T}\right) \tag{2}$$

where A is the junction area, A^{**} is the effective Richardson constant, ϕ_b is the barrier height of the Schottky diode, and $\phi_T = kT/q$. The plots of $\log I$ versus V (in air and in 800-ppm H_2 in N_2 gas) at 450 °C are shown in Fig. 8. The plots show good linearity, which indicates that the conduction mechanism of the samples in both air and hydrogen environment is controlled by the thermionic emission.

Fig. 9 shows the variation of I_{air} as a function of temperature under a fixed electric field (5 MV/cm) in order to take into account the effect of thickness variation among the samples. The I_{air} of all the samples increases with temperature due to thermionic emission. The NO sample has the smallest I_{air}, while the N2 sample has the largest. This should be due to the fact that adding N into the Hf–Ti oxide can result in better bulk and interface qualities and, hence, smaller leakage current [24], [25]. As discussed in [18], NO nitridation is a promising passivation method to improve the electrical properties of high-k devices because, during the nitridation process, nitrogen atoms decomposed from the NO gas can react with the SiC wafer, forming a nitrogen-terminated passivation layer at the surface of the SiC wafer to help remove the dangling bonds there. In addition, the N species can couple with the O vacancies and reduce the interfacial strain, fixed oxide charges, carbon-related interface traps, carbon atoms, and clusters at the interface [26], [27]. The SiON interlayer formed between the high-k

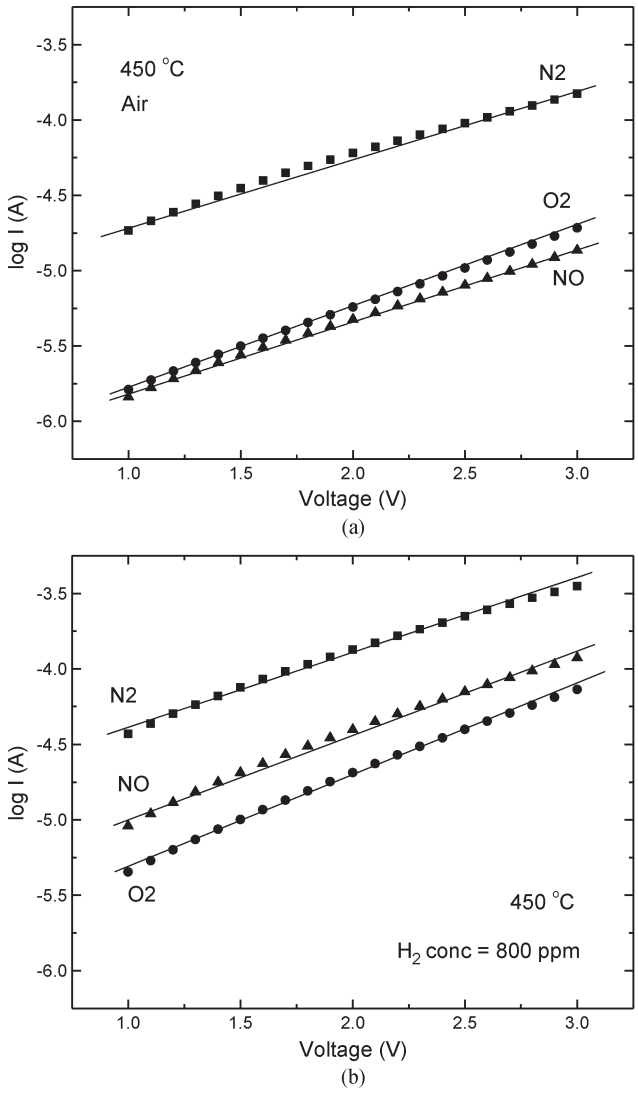

Fig. 8. I–V characteristics of the samples at 450 °C in (a) air and (b) 800-ppm H_2 in N_2.

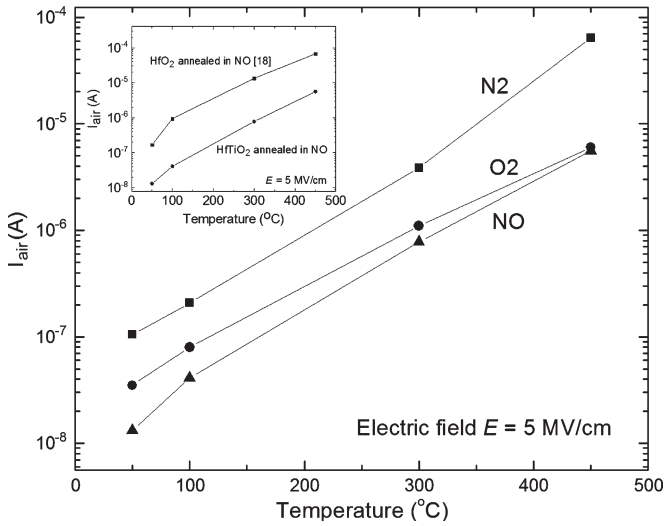

Fig. 9. $I_{\rm air}$ of the samples as a function of temperature. The inset shows a comparison of the $I_{\rm air}$ of the $HfTiO_2$ and HfO_2 samples, both annealed in NO.

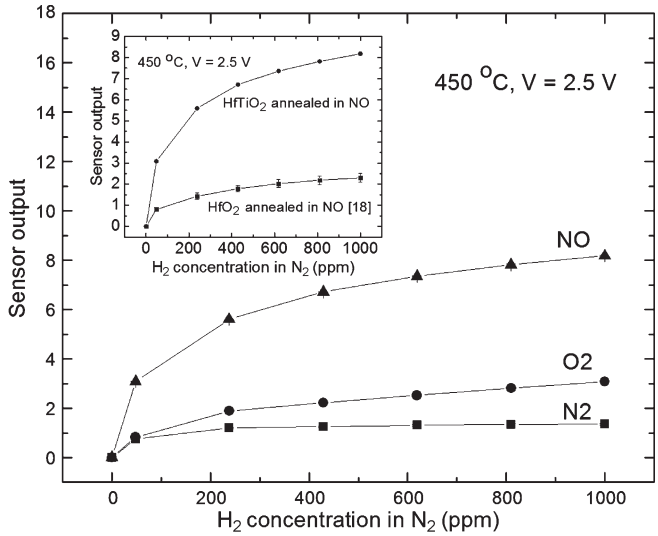

Fig. 10. Sensor outputs of the samples (bias voltage = 2.5 V) upon exposure to different H_2 concentrations in N_2 at 450 °C. The inset shows a comparison of the sensor outputs of the $HfTiO_2$ and HfO_2 samples, both annealed in NO. The standard deviation on the sensor output is 0.014–0.42.

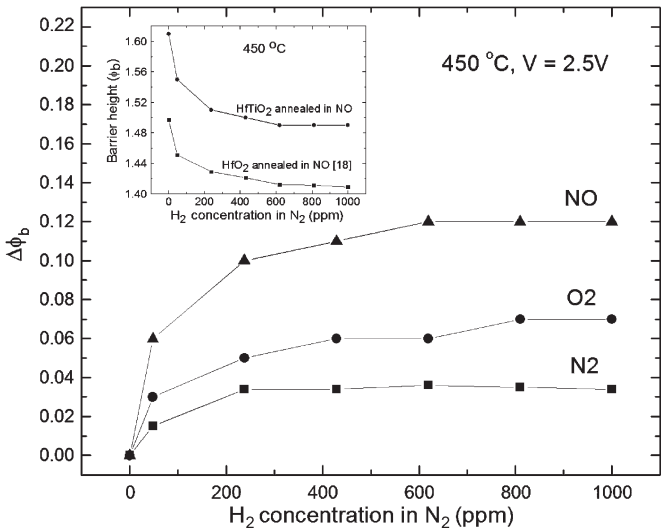

Fig. 11. Barrier-height variations of the $HfTiO_2$ samples annealed in N_2, O_2, and NO upon exposure to different H_2 concentrations in N_2 at 450 °C. The inset shows a comparison of the $HfTiO_2$ and HfO_2 samples, both annealed in NO.

dielectric and the substrate during the NO nitridation process can also improve the interface quality and suppress the leakage associated with high-k materials [24]. The inset of Fig. 9 shows a comparison of the $I_{\rm air}$ of the $HfTiO_2$ and HfO_2 samples both annealed in NO. The $I_{\rm air}$ of the $HfTiO_2$ sample is smaller than that of the HfO_2 sample. This should be attributed to the decrease of conduction-band offset due to the Ti added into the HfO_2 film [28], resulting in a larger barrier height at the Pt/$HfTiO_2$ interface (as shown in the following).

The sensor outputs of the samples upon exposure to different H_2 concentrations are shown in Fig. 10. The sensor output is defined as $(I_{\rm H2} - I_{\rm air})/I_{\rm air}$, where $I_{\rm H2}$ and $I_{\rm air}$ are the currents of the sensors measured in hydrogen and air, respectively. At 450 °C under a forward voltage of 2.5 V, the sensor outputs of all the samples increase with hydrogen concentration. This phenomenon could be explained as follows. When hydrogen

TABLE II
COMPARISON OF METAL–INSULATOR–SEMICONDUCTOR HYDROGEN SENSORS WITH DIFFERENT METAL OXIDES AS GATE INSULATOR

Gate insulator	Insulator thickness (nm)	H_2 concentration (ppm)	Temperature (°C)	Sensor output (%)	Response time (s)
$Ba_{0.67}Sr_{0.33}TiO_3$ [4]	200	1042	205	~40	-
La_2O_3 [10]	4	619	150	~675	-
TiO_2 [12]	5	500	150	~75	~10
Ta_2O_5 [13]	4	5000	150	~22	260
HfO_2 [18]	5.51	800	450	99	2.2
HfON [18]	5.81	800	450	219	10.5
Al_2O_3 (Rh 6 %) [20]	190	1000	100	~29	~600
ZnO [29]	10	1000	25	~329	-
MoO_3 [30]	-	10000	180	~38	40
WO_3 [31]	100	10000	530	~11	-
β-Ga_2O_3 [32]	4	1000	77	~10000	5
$HfTiO_2$ [This work]	4.1	800	450	135	6.9
HfTiON [This work]	4.3	800	450	782	4.6

concentration increases, more hydrogen molecules can be absorbed and decompose into hydrogen atoms at the surface of the Pt electrode, resulting in a stronger polarized layer formed at the metal/insulator interface and, hence, a larger barrier-height reduction, thus resulting in higher sensor output. The N2 sample has a sensor output of 75% at 48-ppm H_2 in N_2, which gets saturated very quickly at around 429 ppm with a value of about 125%. The sensor with NO annealing has higher sensor output than the N_2- or O_2-annealed sensors. At 800 ppm, the sensor output of the NO sample is 5.79 and 2.77 times higher than those of the N2 and O2 samples, respectively. This should be due to the fact that incorporating N into the $HfTiO_2$ film by NO nitridation can passivate its oxygen vacancies and bond to its interstitial oxygen, resulting in fewer interface states, less oxide charges, and better interfacial diffusion barriers. As a result, $I_{\rm air}$ is significantly reduced as shown in Fig. 9 (91% and 7% reductions compared with the N2 and O2 samples, respectively), and hence, the sensor output is increased. In addition, the sensor output of the O2 sample is higher than that of the N2 sample. This may be due to the fact that O_2 annealing can improve the stoichiometry of the high-k film, thus reducing $I_{\rm air}$ significantly (90% reduction compared with the N2 sample). In the inset of Fig. 10, the sensor output of the $HfTiO_2$ sample annealed in NO is compared with that of its counterpart based on HfO_2. The sensor output of the $HfTiO_2$ sample is 3.5 times higher than that of the HfO_2 sample, and the $I_{\rm air}$ of the $HfTiO_2$ sample is 11.89 times smaller than that of the HfO_2 sample (as shown in the inset of Fig. 9). This could be explained by the fact that the conduction-band offset decreases after Ti doping, thus increasing the metal/insulator barrier height and suppressing $I_{\rm air}$, resulting in higher sensor output. The response/recovery time defined as the time required to reach e^{-1} of the final steady-state value can be obtained from the transient measurements. The response (recovery) times for the N2, O2, and NO samples are 6.9 (13.7), 13.6 (15), and 4.6 (15) s, respectively. The recovery time is longer than the response time, indicating that more time is needed for the H atoms to diffuse out of the Pt/$HfTiO_2$ interface to the Pt surface and then recombine together to form H_2 gas.

Fig. 11 shows the change in the barrier height of the samples upon exposure to different H_2 concentrations. From (2), the barrier height ϕ_b can be calculated using the following formula:

$$\phi_b = -\phi_T \ln\left(\frac{I_o}{AA^{**}T^2}\right). \tag{3}$$

When hydrogen concentration increases, the barrier height of the sensor decreases, and the barrier-height lowering defined as $\phi_b\ (\text{air}) - \phi_b\ (\text{H}_2)$ increases. It is because, when more hydrogen molecules dissociate at the front electrode, more hydrogen atoms can be adsorbed at the electrode–insulator interface to form a stronger polarized layer, causing a larger barrier-lowering effect. Upon hydrogen exposure, the NO sample gives the largest change in barrier height among the test samples and, hence, the highest sensor output. The inset of Fig. 11 shows a comparison of the barrier heights of the $HfTiO_2$ and HfO_2 samples. The ϕ_b (air) of the $HfTiO_2$ sample is 1.61 V, while that of the HfO_2 sample is 1.48 V. Incorporating Ti into the HfO_2 film increases ϕ_b possibly due to the reduction of the conduction-band offset, as mentioned earlier. Therefore, the enhanced sensor output of the $HfTiO_2$ sample should be mostly due to the larger barrier height at the Pt/$HfTiO_2$ interface which greatly reduces $I_{\rm air}$. Table II compares the metal–insulator–semiconductor-based hydrogen sensors with different metal oxide insulators reported in the literature. As compared with previous results, the proposed $HfTiO_2$ sensor exhibits high sensor output and fast response at high operating temperature, suggesting that the hydrogen sensor in this study has promising applications for detecting hydrogen leakage in harsh environments.

IV. CONCLUSION

Hafnium titanate ($HfTiO_2$) is successfully used as the gate insulator for fabricating MISiC Schottky-diode hydrogen sensors. The effects of different annealing gases (N_2, O_2, and NO) on the sensing characteristics of the device have been studied. Experimental results demonstrate that the sensors have high sensor output at high operating temperature. Among the three sensors, the sensor with NO annealing has the smallest $I_{\rm air}$ and the highest sensor output. This should be attributed to the incorporation of nitrogen in the device which can strongly bond to the interstitial oxygen, forming less mobile NO^- molecules, resulting in better insulator and insulator/substrate interface quality and, hence, better sensor performance. The study also finds that O_2 annealing can improve the film stoichiometry to give smaller $I_{\rm air}$ and, hence, higher sensor output when compared to N_2 annealing. Compared to the HfO_2 sensor, the proposed $HfTiO_2$ sensor produces a sensor output increased by a factor of 3.6. This improved performance is attributed to a larger energy barrier at the Pt/$HfTiO_2$ interface which reduces the leakage current of the device. It is also found that

the electrical conduction of the sensors is controlled by the thermionic-emission mechanism. In summary, these sensors have potential applications for detecting hydrogen leakage, particularly in high-temperature environments.

REFERENCES

[1] F. McMurry, *Chemistry*, 4th ed. Englewood Cliffs, NJ: Prentice-Hall, ch. 14.

[2] W. H. Brattain and J. Bardeen, "Surface properties of germanium," *Bell Syst. Tech. J.*, vol. 32, no. 1, pp. 1–41, Jan. 1953.

[3] I. Lundstrom, S. Shivaraman, C. Svensson, and L. Lundkvist, "A hydrogen-sensitive MOS field effect transistor," *Appl. Phys. Lett.*, vol. 26, no. 2, pp. 55–57, Jan. 1975.

[4] X. F. Chen, W. G. Zhu, and O. K. Tan, "Microstructure, dielectric properties and hydrogen gas sensitivity of sputtered amorphous $Ba_{0.67}Sr_{0.33}TiO_3$ thin films," *Mater. Sci. Eng., B*, vol. 77, no. 2, pp. 177–184, Aug. 2000.

[5] A. Trinchi, K. Galatsis, W. Wlodarski, and Y. X. Li., "A Pt/Ga_2O_3-ZnO/SiC Schottky diode-based hydrocarbon gas sensor," *IEEE Sensors J.*, vol. 3, no. 5, pp. 548–553, Oct. 2003.

[6] J. P. Xu, P. T. Lai, D. G. Zhong, and C. L. Chan, "Improved hydrogen-sensitive properties of MISiC Schottky sensor with thin NO-grown oxynitride as gate insulator," *IEEE Trans. Electron Devices*, vol. 24, no. 1, pp. 13–15, Jan. 2003.

[7] W. M. Tang, C. H. Leung, P. T. Lai, and J. P. Xu, "A comparison of MISiC Schottky-diode hydrogen sensors made by NO, N_2O, or NH_3 nitridations," *IEEE Trans. Electron Devices*, vol. 53, no. 9, pp. 2378–2383, Sep. 2006.

[8] E. P. Cusev, M. Copel, E. Cartier, I. J. R. Baumvol, C. Krug, and M. A. Gribelyuk, "High-resolution depth profiling in ultrathin Al_2O_3 film on Si," *Appl. Phys. Lett.*, vol. 76, no. 2, pp. 176–178, Nov. 2000.

[9] M. Gurvitch, L. Manchanda, and J. M. Gibson, "Study of thermally oxidized yttrium films on silicon," *Appl. Phys. Lett.*, vol. 51, no. 12, pp. 919–921, Sep. 1987.

[10] G. Chen, P. T. Lai, and J. Yu, "A study on metal–insulator–silicon hydrogen sensor with La_2O_3 as gate insulator," in *Proc. 10th IEEE ICSICT*, 2010, pp. 1465–1467.

[11] M. Copel, M. A. Gribelyuk, and E. Gusev, "Structure and stability of ultrathin zirconium oxide layers on Si (001)," *Appl. Phys. Lett.*, vol. 76, no. 4, pp. 436–438, Jan. 2000.

[12] T. H. Chou, Y. K. Fang, Y. T. Chiang, K. C. Lin, C. Lin, C. H. Kao, and H. Y. Lin, "The Pd/TiO_2/n-LTPS thin-film Schottky diode on glass substrate for hydrogen sensing applications," *IEEE Electron Device Lett.*, vol. 29, no. 11, pp. 1232–1235, Nov. 2008.

[13] J. Yu, G. Chen, C. X. Li, M. Shafiei, J. Z. Ou, J. du Plessis, K. Kalantar-zadeh, P. T. Lai, and W. Wlodarski, "Hydrogen gas sensing properties of Pt/Ta_2O_5 Schottky diodes based on Si and SiC substrates," *Sens. Actuators A, Phys.*, vol. 172, no. 1, pp. 9–14, Dec. 2011.

[14] W. M. Tang, C. H. Leung, and P. T. Lai, "Effects of N_2-annealing conditions on the sensing properties of Pt/HfO_2/SiC Schottky-diode hydrogen sensor," *Thin Solid Films*, vol. 519, no. 1, pp. 505–511, Oct. 2010.

[15] J. Mcpherson, J. Kim, A. Shanware, H. Mogual, and J. Rodriguez, "Proposal universal relationship between dielectric breakdown and dielectric constant," in *Proc. IEDM*, 2002, pp. 633–636.

[16] M. Li, Z. Zhang, S. A. Campbell, W. L. Gladfelter, M. P. Agustin, D. O. Klenov, and S. Stemmer, "Electrical and material characterizations of high-permittivity $Hf_xTi_{1-x}O_2$ gate insulators," *J. Appl. Phys.*, vol. 98, no. 5, pp. 054506-1–054506-8, Sep. 2005.

[17] W. M. Tang, K. H. Cheng, C. H. Leung, P. T. Lai, J. P. Xu, and C. M. Che, "Improved performance for OTFT with $HfTiO_2$ as gate dielectric by N_2O annealing," in *Proc. IEEE Int. Conf. Electron Devices Solid-State Circuits*, 2007, pp. 189–192.

[18] W. M. Tang, C. H. Leung, and P. T. Lai, "Enhanced sensing performance of MISiC Schottky-diode hydrogen sensor by using HfON as gate insulator," *IEEE Sensors J.*, vol. 11, no. 11, pp. 2940–2946, Nov. 2011.

[19] T. Y. Chen, H. I. Chen, C. C. Huang, C. S. Hsu, P. S. Chiu, P. C. Chou, and W. C. Liu, "Improved hydrogen-sensing performance of a Pd/GaN Schottky diode with a surface plasma treatment approach," *Sens. Actuators B, Chem.*, vol. 159, no. 1, pp. 159–162, Nov. 2011.

[20] A. Ryzhikov, F. Robaut, M. Labeau, and A. Gaskov, "New gas sensitive MIS structures Pt/Al_2O_3 (M = Pt, Rh)/Si with a granular dielectric layer," *Sens. Actuators B, Chem.*, vol. 133, no. 2, pp. 613–616, Aug. 2008.

[21] H. Hu, C. X. Zhu, Y. F. Lu, Y. H. Wu, T. Liew, M. F. Li, B. J. Cho, W. K. Choi, and N. Yakovlev, "Physical and electrical characterization of HfO_2 metal–insulator–metal capacitors for Si analog circuit applications," *J. Appl. Phys.*, vol. 94, no. 1, pp. 551–557, Jul. 2003.

[22] C. Wang, L. Fang, G. Zhang, D. M. Zhuang, and M. S. Wu, "I–V characteristics of tantalum oxide film and the effect of defects on its electrical properties," *Thin Solid Films*, vol. 458, no. 1/2, pp. 246–250, Jun. 2004.

[23] D. K. Schroder, *Semiconductor Material and Device Characterization,* 3rd ed. Piscataway, NJ: Wiley, 2006.

[24] L. M. Lin and P. T. Lai, "Improved high-field reliability for a SiC metal–oxide–semiconductor device by the incorporation of nitrogen into its HfTiO gate dielectric," *J. Appl. Phys.*, vol. 102, no. 5, pp. 054515-1–054515-5, Sep. 2007.

[25] C. X. Li, P. T. Lai, and J. P. Xu, "Improved reliability of Ge MOS capacitor with HfTiON high-k dielectric by using Ge surface pretreatment in wet NO," *Microelectron. Eng.*, vol. 84, no. 9/10, pp. 2340–2343, Sep. 2007.

[26] G. Y. Chung, C. C. Tin, J. R. Williams, K. McDonald, M. Di Ventra, S. T. Pantelides, L. C. Feldman, and R. A. Weller, "Effect of nitric oxide annealing on the interface trap densities near the band edges in the 4H polytype of silicon carbide," *Appl. Phys. Lett.*, vol. 76, no. 13, pp. 1713–1715, Mar. 2000.

[27] P. Tanner, S. Dimitrijev, H. F. Li, D. Sweatman, K. E. Prince, and H. B. Harrison, "SIMS analysis of nitride oxides grown on 4H–SiC," *J. Electron. Mater.*, vol. 28, no. 2, pp. 109–111, 1999.

[28] M. Liu, L. D. Zhang, G. He, X. J. Wang, and M. Fang, "Effect of Ti incorporation on the interfacial and optical properties of HfTiO thin films," *J. Appl. Phys.*, vol. 108, no. 2, pp. 024102-1–024102-4, Jul. 2010.

[29] H. Y. Lee, H. L. Huang, and C. T. Lee, "Hydrogen sensing performances of Pt/i-ZnO/GaN metal–insulator–semiconductor diodes," *Sens. Actuators B, Chem.*, vol. 157, no. 2, pp. 460–465, Oct. 2011.

[30] J. Yu, S. J. Ippolito, M. Shafiei, D. Dhawan, W. Wlodarski, and K. K. Zadeh, "Reverse biased Pt/nanostructured MoO_3/SiC Schottky diode based hydrogen gas sensors," *Appl. Phys. Lett.*, vol. 94, no. 1, pp. 013504-1–013504-3, Jan. 2009.

[31] S. Kandasamy, A. Trinchi, W. Wlodarski, E. Comini, and G. Sberveglieri, "Hydrogen and hydrocarbon gas sensing performance of Pt/WO_3/SiC MROSiC devices," *Sens. Actuators B, Chem.*, vol. 111/112, pp. 111–116, Nov. 2005.

[32] C. T. Lee and J. T. Yan, "Sensing mechanisms of Pt/β-Ga_2O_3/GaN hydrogen sensor diodes," *Sens. Actuators B, Chem.*, vol. 147, no. 2, pp. 723–729, Jun. 2010.

W. M. Tang received the B.Eng., M.Phil., and Ph.D. degrees in electrical and electronic engineering from The University of Hong Kong, Pokfulam, Hong Kong.

She is currently a Postdoctoral Scholar with Stanford University, Stanford, CA.

C. H. Leung received the Ph.D. degree in electrical engineering from The University of Hong Kong, Pokfulam, Hong Kong.

Since 1986, he has been teaching at the Department of Electrical and Electronic Engineering, The University of Hong Kong.

P. T. Lai (M'90–SM'04) received the B.Sc.(Eng.) degree from The University of Hong Kong, Pokfulam, Hong Kong.

He is currently a Professor with the Department of Electrical and Electronic Engineering, The University of Hong Kong.